مجلة الريادة للبحوث والأنشطة العلمية
Al-Riyadah Journal For Researches And Scientific Activities
العدد الرابع عشر
published 1-8-2026 تاريخ النشر Accepted 22-7-2026 تاريخ القبول Received 5-7-2026 تاريخ الاستلام

Thermoelastic Analysis of a Rotating Half-Space with Temperature-Dependent Properties Under Laser Pulse Heating using Green–Naghdi Type II and Type III Models

Alzaerah R. M. Aldeeb[1], **Mohamed I. A. Othman**[2,*]

[1]**Department of Mathematics, faculty of education Alzawia University,Libya**

[2]**Department of Mathematics, Faculty of Science, Zagazig University, 44519, Zagazig, Egypt**

Email:a.aldeeb@zu.edu.ly,_78 @yahoo.com, *m_i_a_othman@yahoo.com

https://orcid.org/0009-0007-5338-7156 .. ORCID 0000-0002-9577-5479

Abstract:

This study presents a theoretical investigation of generalized thermoelastic wave propagation in a rotating isotropic half-space subjected to ultra-short laser pulse heating, considering temperature-dependent material properties. The mathematical model is formulated within the framework of the Green–Naghdi (GN) theories of Type II and Type III. The governing equations are solved analytically using the normal mode method to obtain closed-form solutions for the temperature distribution, displacement components, and stress fields. Numerical simulations are performed, and the resulting thermoelastic fields are illustrated graphically to evaluate the influences of rotation, temperature-dependent properties, and laser pulse characteristics. A comparative analysis between the GN-II and GN-III models is carried out to highlight the differences between non-dissipative thermal wave propagation and thermally dissipative behavior. Furthermore, the thermoelastic response is examined at two different time instants to demonstrate the combined effects of laser pulse heating, rotational motion, and variable material properties on wave propagation and stress distribution. The results provide valuable insights into the thermoelastic behavior of rotating media exposed to laser irradiation and contribute to the understanding of heat-induced mechanical responses in advanced engineering materials.

Keywords: Generalized thermoelasticity, Green-Naghdi theory, Rotation, Laser pulse, Temperature-dependent properties, Normal mode analysis.

مجلة الريادة للبحوث والأنشطة العلمية
Al-Riyadah Journal For Researches
And Scientific Activities
العدد الرابع عشر
published 1-8-2026 تاريخ النشر Accepted 22-7-2026 تاريخ القبول Received 5-7-2026 تاريخ الاستلام

"التحليل الحراري المرن لنصف فضاء دوار بخصائص تعتمد على درجة الحرارة تحت تسخين نبضات الليزر باستخدام نماذج غرين–ناغدي من النوع الثاني والثالث"

الملخص:

تقدم هذه الدراسة بحثًا نظريًا حول انتشار الموجات الحرارية المرنة المعممة في نصف فضاء متجانس دوار معرض لتسخين بنبضات ليزر قصيرة جدا، مع مراعاة خصائص المادة المعتمدة على درجة الحرارة. تمت صياغة النموذج الرياضي في إطار نظريات غرين–ناغدي (GN) من النوع الثاني والثالث. تم حل المعادلات الحاكمة تحليليًا باستخدام طريقة الوضع الطبيعي للحصول على حلول مغلقة لتوزيع درجة الحرارة ومكونات الإزاحة ومجالات الإجهاد تُجرى عمليات محاكاة عددية، ويتم توضيح الحقول الحرارية المرنة الناتجة بيانيًا لتقييم تأثيرات الدوران والخصائص المعتمدة على درجة الحرارة وخصائص نبضة الليزر. يتم إجراء تحليل مقارن بين نموذجي GN–II و GN–III لتسليط الضوء على الاختلافات بين انتشار الموجة الحرارية غير المبددة والسلوك الحراري المبدد. علاوة على ذلك، يتم فحص الاستجابة الحرارية المرنة في لحظتين زمنيتين مختلفتين لإظهار التأثيرات المشتركة لتسخين نبضة الليزر والحركة الدورانية وخصائص المواد المتغيرة على انتشار الموجة وتوزيع الإجهاد. توفر النتائج رؤى قيمة حول السلوك الحراري المرن للوسائط الدوارة المعرضة لإشعاع الليزر وتساهم في فهم الاستجابات الميكانيكية الناتجة عن الحرارة في المواد الهندسية المتقدمة.

الكلمات المفتاحية: المرونة الحرارية المعممة، نظرية غرين–ناغدي، الدوران، الليزر

1. Introduction

The primary objective of this study is to investigate the generalized thermoelastic response of a rotating homogeneous isotropic half-space subjected to ultra-short pulsed laser heating while accounting for temperature-dependent material properties. The analysis is carried out within the framework of the Green–Naghdi Type II (GN-II) and Type III (GN-III) thermoelastic theories.Othman et al. [1] studied the effect of initial stress on generalized thermoelastic medium with three-phase-lag model under temperature-dependent properties.

Ultra-short pulsed lasers, with pulse durations ranging from nanoseconds to femto-seconds, generate extremely high heating rates and induce rapid transient thermo-elastic

مجلة الريادة للبحوث والأنشطة العلمية
Al-Riyadah Journal For Researches And Scientific Activities
العدد الرابع عشر
published 1-8-2026 تاريخ النشر Accepted 22-7-2026 تاريخ القبول Received 5-7-2026 تاريخ الاستلام

waves. Under such conditions, the classical coupled thermoelasticity theory becomes inadequate because it predicts an infinite speed of heat propagation, which is physically unrealistic. This limitation has motivated the development of generalized thermoelastic theories incorporating finite thermal wave speeds, as discussed by Hetnarski and Eslami [2]. The present work employs the Green–Naghdi formulations to provide a more realistic description of thermoelastic wave propagation in rotating media subjected to laser pulse heating.Othman and Said [3] investigated the effect of rotation on two-dimensional problem of a fiber-reinforced thermoelastic with one relaxation time.Othman et al. [4] applied an eigenvalue-based method to evaluate the combined effects of fiber reinforcement, viscoelasticity, rotation, and initial stress in magneto-thermoelastic media. To overcome the shortcomings of the classical thermoelasticity theory, several generalized thermoelastic models have been developed to account for finite thermal wave propagation. Among these, the Green–Naghdi (GN) theories have received considerable attention due to their sound thermodynamic foundation and broad applicability. Green and Naghdi first introduced the GN formulations in their seminal paper A Re-Examination of the Basic Postulates of Thermomechanics, in which the Type II (GN-II) and Type III (GN-III) theories were established. They subsequently presented the GN-II model in thermoelasticity without energy dissipation, which describes thermal wave propagation in the absence of energy dissipation, whereas the GN-III model incorporates thermal damping effects [5, 6].

Since then, numerous researchers have extended the Green–Naghdi theories to investigate various thermoelastic problems. Abbas investigated generalized thermo-elastic wave propagation in an infinite medium using the GN theory. Hobiny and Abbas [7,8] analyzed the GN-II and GN-III models for porous media subjected to thermal shock loading. Singh and Kaur [9] examined the influence of rotation on generalized thermoelastic responses, while Abo-Dahab [10] studied the combined effects of rotation and initial stress within the Green–Naghdi framework. Lotfy and El-Bary [11] investigated generalized thermoelastic media with rotation and temperature-dependent material properties. Zenkour [12] analyzed thermoelastic interactions in rotating media with temperature-dependent properties based on the GN theory. Sherief and El-Sayed [13] developed a two-temperature Green–Naghdi model for thermoelastic analysis, and Lata and Kaur [14]

published 1-8-2026 تاريخ النشر Accepted 22-7-2026 تاريخ القبول Received 5-7-2026 تاريخ الاستلام

examined the combined effects of magnetic fields and rotation on generalized thermoelastic solids.

These studies demonstrate the versatility of the Green–Naghdi formulations in modeling thermoelastic wave propagation under various physical conditions. However, the combined effects of ultra-short laser pulse heating, rotation, and temperature-dependent material properties within the GN-II and GN-III frameworks have received comparatively limited attention, providing the motivation for the present investigation.

Several researchers have also investigated thermoelastic problems involving laser-induced thermal loading. Youssef and Al-Lehaibi[15] studied the generalized thermoelastic response of a solid sphere subjected to laser pulse heating. Mondol and Mukhopadhyay[16] analyzed the thermoelastic behavior of a rotating elastic medium under laser pulse excitation. Sharma and Grover [17] presented a thermoelastic analysis of rotating disks exposed to laser heating, while Kumar and Devi [18] examined the effects of laser pulse loading on generalized thermoelastic media within the framework of the Green–Naghdi Type III theory. Othman and Kumar [19] investigated the response of thermoelastic solids subjected to laser-induced thermal loading using the GN-III model. In a related study, Ezzat[20] analyzed magneto-thermoelastic problems involving thermoelectric effects and memory-dependent derivatives.

The above review demonstrates that significant progress has been made in the analysis of generalized thermoelasticity under the influences of rotation, laser pulse heating, and temperature-dependent material properties. However, the combined effects of these factors within the frameworks of the Green–Naghdi Type II (GN-II) and Type III (GN-III) theories have not been comprehensively investigated. Therefore, the present study aims to analyze generalized thermoelastic wave propagation in a rotating isotropic half-space with temperature-dependent material properties subjected to ultra-short laser pulse heating. A comparative investigation between the GN-II and GN-III models is carried out to evaluate the influences of thermal dissipation, rotational motion, and variable material properties on the thermo- elastic response.

The novelty of the present study lies in the comprehensive investigation of generalized thermoelastic wave propagation in a rotating isotropic half-space subjected to ultra-short laser pulse heating while simultaneously accounting for temperature-dependent material

مجلة الريادة للبحوث والأنشطة العلمية
Al-Riyadah Journal For Researches And Scientific Activities
العدد الرابع عشر
published 1-8-2026 تاريخ النشر   Accepted 22-7-2026 تاريخ القبول   Received 5-7-2026 تاريخ الاستلام

properties within the frameworks of the Green–Naghdi Type II (GN-II) and Type III (GN-III) thermoelastic theories. Although these aspects have been studied individually in previous investigations, their combined effects have received limited attention.

2. Formulation of the problem and governing equations

The present study deals with a homogeneous and isotropic half-space, where $(z \geq 0)$, characterized by material properties that depend on temperature. The bounding plane at $z = 0$ is exposed to a thermal load induced by a laser pulse.

The problem is analyzed under the condition of plane strain in the *xz*-plane. The displacement vector is represented as $u_i = (u_1, 0, u_3)$, where $i = 1, 3$.

It is assumed that the entire medium rotates with a constant angular velocity $\boldsymbol{\Omega} = \Omega \boldsymbol{n}$, where $\boldsymbol{n}$ denotes the unit vector along the axis of rotation. In a rotating frame of reference, the equation of motion includes two extra inertial terms as discussed by Schoenberg and Censor[21]: the centripetal acceleration term $\boldsymbol{\Omega} \times (\boldsymbol{\Omega} \times \boldsymbol{u})$ and the Coriolis acceleration term $2\boldsymbol{\Omega} \times \dot{\boldsymbol{u}}$.

Building on the equation of motion derived previously, the field equations for a thermoplastic solid in a rotating frame can be expressed in terms of displacement and temperature. Under the plane strain assumption in the *xz*-plane, and considering temperature-dependent material constants, the coupled equations of motion in the x and z directions take the following form(Othman and Abd-Elaziz [22]):

$$\sigma_{ij,j} = \rho[\ddot{u}_i + \{\boldsymbol{\Omega} \times \boldsymbol{\Omega} \times \boldsymbol{u}\}_i + 2(\boldsymbol{\Omega} \times \dot{\boldsymbol{u}})_i], \quad i, j = 1, 3. \tag{1}$$

$$\mu \nabla^2 u_1 + (\lambda + \mu)\frac{\partial e}{\partial x} - \beta \nabla \frac{\partial T}{\partial x} = \rho[\ddot{u}_1 - \Omega^2 u_1 - 2\Omega \dot{u}_3], \tag{2}$$

$$\mu \nabla^2 u_3 + (\lambda + \mu)\frac{\partial e}{\partial z} - \beta \nabla \frac{\partial T}{\partial z} = \rho[\ddot{u}_3 - \Omega^2 u_3 + 2\Omega \dot{u}_1], \tag{3}$$

For the thermal field, the heat conduction equation is formulated based on Green-Naghdi theories. The general expression accounting for thermal conductivity and energy dissipation is given by(Othman and Atwa [23]):

$$K \nabla^2 T + k^* \nabla^2 \frac{\partial T}{\partial t} = \rho C_E \frac{\partial^2 T}{\partial t^2} + \beta T_0 \frac{\partial^2 e}{\partial e^2} - \rho \frac{\partial Q}{\partial t}. \tag{4}$$

The components of stress tensor are

published 1-8-2026 تاريخ النشر Accepted 22-7-2026 تاريخ القبول Received 5-7-2026 تاريخ الاستلام

$$\sigma_{xx} = \lambda(\frac{\partial u_1}{\partial x} + \frac{\partial u_3}{\partial z}) + \mu \frac{\partial u_1}{\partial x} - \beta T, \tag{5}$$

$$\sigma_{zz} = \lambda(\frac{\partial u_1}{\partial x} + \frac{\partial u_3}{\partial z}) + \mu \frac{\partial u_1}{\partial z} - \beta T, \tag{6}$$

$$\sigma_{xz} = \lambda(\frac{\partial u_1}{\partial z} + \frac{\partial u_3}{\partial x}). \tag{7}$$

In the above relation, the following symbols are used σ_{ij} and e_{ij} denote the components of stress and strain tensors, respectively. The tensor ω_{ij} represents rotation, while $e = e_{kk}$ stands for the volumetric expansion. δ_{ij} is Kronecker's delta, u_i represents the displacement vector. The material constant λ, μ are lame's elastic parameters., T is the absolute temperature, T_0 is the reference temperature in the unreformed state with the assumption that $|(T - T_0)/T_0| < 1$. The symbols ε_0, μ_0 refer to the permittivity and permeability of free space, respectively. The thermo-elastic coupling parameter is given by $\beta = (3\lambda + 2\mu)\alpha_t$, where α_t is the coefficient of linear thermal expansion. ρ denotes the mass density. K and k^* represent the thermal conductivity coefficients associated with GN-II and GN-III models, respectively. C_E denotes the specific heat at constant strain Q is the heat source due to laser pulse.

The Laplacian operator ∇^2 is defend as:

$$\nabla^2 = \frac{\partial^2}{\partial x^2} + \frac{\partial^2}{\partial y^2} + \frac{\partial^2}{\partial z^2}. \tag{8}$$

It is importation to note that when $k^* \to 0$, then Eq. (4) reduces to the heat conduction equation of the GN-II model, $\nabla = \frac{\partial}{\partial x} i + \frac{\partial}{\partial z} k$, and $\nabla^2 = \frac{\partial^2}{\partial x^2} + \frac{\partial^2}{\partial z^2}$.

The surface of the plate is subjected to thermal loading due to laser beam.

The volumetric heat generation Q is modeled as a separable function of time , spas, and depth(Sarkar et al. [24], Othman and Eldeeb [25]):

$$Q = I_0 f(t) g(x) h(z). \tag{9}$$

Here, denotes the maximum intensity of the incident laser beam.

published 1-8-2026 تاريخ النشر Accepted 22-7-2026 تاريخ القبول Received 5-7-2026 تاريخ الاستلام

The time-dependent part $f(t)$ is chosen to model a short laser pulse with a finite rise time. It is taken in the form:

$$f(t) = \frac{t}{t_0^2}\exp(\frac{-t}{t_0}) \tag{10}$$

where t_0 represents the characteristic pulse rise time.

For the spatial distribution along the x-axis, a Gaussian profile is adopted. This gives:

$$g(x) = \frac{1}{2\pi r^2}\exp(\frac{-x^2}{r^2}) \tag{11}$$

In this expression, r is the laser beam radius that controls the width of the heated region. The function $h(z)$ describes the absorption of laser energy within the material and is often taken as an exponential decay. For surface heating, it can be approximated as

$$h(z) = \gamma e^{-\gamma z} \tag{12}$$

where γ is the absorption coefficient of the medium.

Substituting Eqs. (10)-(12) into Eq. (9) we get

$$Q = \frac{I_0\gamma}{2\pi r^2 t_0^2} t \exp(\frac{-x^2}{r^2} - \frac{t}{t_0})\exp(-\gamma z). \tag{13}$$

In this analysis, the effect of temperature variation on the elastic modulus is considered while other thermo-physical properties are assumed constant. To incorporate this, the material constants are taken as functions of temperature through a non-dimensional function $f(t)$ as follows(Othman and Eldeeb [26]):

$$\lambda = \lambda_0 f(T),\ \ \mu = \mu_0 f(T),\ \ \beta = \beta_0 f(T),\ \ \alpha = \alpha_0 f(T),\ \ \xi = \xi_0 f(T),$$

$$k = k_0 f(T),\qquad \omega_0 = \omega_{10} f(T). \tag{14}$$

Where $\lambda_0, \mu_0, \beta_0, \alpha_0, \xi_0, \omega_{10}, k_0,$ are constants evaluated at the reference temperature T_0. For the special case of temperature-independent properties, we set $f(T) = 1$. A common linear approximation for $f(T)$ is given by $f(T) = (1 - \alpha^* T_0)$, where α^* is the temperature coefficient.

To simplify the governing equations, a set of dimensionless variables is introduced. These are defined using characteristic quantities of the problem as:

published 1-8-2026 تاريخ النشر Accepted 22-7-2026 تاريخ القبول Received 5-7-2026 تاريخ الاستلام

$$(x',z') = \frac{\omega_1^*}{c_0}(x,z),\ (u_1',u_3') = \frac{\omega_1^*}{c_1}(u_1,u_3),\ \sigma_{ij}' = \frac{\sigma_{ij}}{\mu_0}\sigma_{ij},\ T' = \frac{T}{T_0},\ t' = \omega_1^* t,$$

$$\Omega' = \frac{\Omega}{\omega_1^*},\ c_1^2 = \frac{\lambda_0 + 2\mu_0}{\rho},\ \omega_1^* = \frac{\rho C_E c_1^2}{k},\ p' = \frac{p}{\mu},\ Q' = \frac{Q}{\omega_1^* T_0 C_E}. \tag{15}$$

From Eq. (15) in to Eqs. (2)-(4) we get

$$\nabla^2 u_1 + E_1 \frac{\partial e}{\partial x} - E_2 \frac{\partial T}{\partial x} = E_3 [\frac{\partial^2 u_1}{\partial t^2} - \Omega^2 u_1 - 2\Omega \frac{\partial u_3}{\partial t}], \tag{16}$$

$$\nabla^2 u_3 + E_1 \frac{\partial e}{\partial z} - E_2 \frac{\partial T}{\partial z} = E_3 [\frac{\partial^2 u_3}{\partial t^2} - \Omega^2 u_3 + 2\Omega \frac{\partial u_1}{\partial t}], \tag{17}$$

$$\varepsilon_3 \nabla^2 T + \varepsilon_2 \frac{\partial}{\partial t} \nabla^2 T = \frac{\partial^2 \mathrm{T}}{\partial t^2} + \varepsilon_1 \frac{\partial^2 e}{\partial t^2} - E_4 \frac{\partial e}{\partial t} Q. \tag{18}$$

Also, the constitutive relations (5)-(7) reduces to

$$\sigma_{xx} = E_5 (\frac{\partial u_1}{\partial x} + \frac{\partial u_3}{\partial z}) + \frac{2}{A^*} \frac{\partial u_1}{\partial x} - E_6 T, \tag{19}$$

$$\sigma_{zz} = E_5 (\frac{\partial u_1}{\partial x} + \frac{\partial u_3}{\partial z}) + \frac{2}{A^*} \frac{\partial u_3}{\partial z} - E_6 \mathrm{T}, \tag{20}$$

$$\sigma_{xz} = \frac{1}{A^*} (\frac{\partial u_1}{\partial z} + \frac{\partial u_3}{\partial x}). \tag{21}$$

Where $E_1 = \frac{\lambda_0 + \mu_0}{\mu_0}$, $E_2 = \frac{\beta_0 T_0}{\mu_0}$, $E_3 = \frac{A^* \rho c_1^2}{\mu_0}$, $E_4 = \frac{K_0 \omega_1^*}{A^* \rho c_1^2 ce}$, $E_5 = \frac{\lambda_0}{A^* \mu_0}$,

$E_6 = \frac{\beta_0 T_0}{A^* \mu_0}$, $\varepsilon_1 = \frac{\beta_0}{A^* \rho ce}$ $\varepsilon_2 = \frac{K^* \omega_1^*}{A^* \rho c_1^2 ce}$, $\varepsilon_3 = \frac{K_0}{A^* c_1^2 \rho ce}$, $A^* = \frac{1}{F(T)} = \frac{1}{1 - \alpha^* T_0}$.

Also $\varepsilon_1, \varepsilon_2$ and ε_3 are the coupling constants. Using the expression relating displacement components $u_1(x, z, t)$ and $u_3(x, z, t)$ to the scalar potential functions $\psi_1(x, z, t)$ and $\psi_2(x, z, t)$ in dimensionless form

$$u_1 = \frac{\partial \psi_1}{\partial x} + \frac{\partial \psi_2}{\partial z}, \text{ and } \quad u_3 = \frac{\partial \psi_1}{\partial z} - \frac{\partial \psi_2}{\partial x}, \tag{22}$$

$$e = \nabla^2 \psi_1, \quad \text{and} \quad (\frac{\partial u_1}{\partial z} - \frac{\partial u_3}{\partial x}) = \nabla^2 \psi_2. \tag{23}$$

By substituting from Eq. (22) in Eqs. (16)-(18), this yields

مجلة الريادة للبحوث والأنشطة العلمية
Al-Riyadah Journal For Researches And Scientific Activities
العدد الرابع عشر
published 1-8-2026 تاريخ النشر Accepted 22-7-2026 تاريخ القبول Received 5-7-2026 تاريخ الاستلام

$$[\,(1+E_1)\nabla^2 - E_3(\frac{\partial^2}{\partial t^2} - \Omega^2)]\psi_1 - 2E_3\Omega\psi_2 - E_2 T = 0, \tag{24}$$

$$2E_3\Omega\frac{\partial\psi_1}{\partial t} + [\nabla^2 + E_3(\frac{\partial^2}{\partial t^2} - \Omega^2)]\psi_2 = 0, \tag{25}$$

$$\varepsilon_3\nabla^2 T + \varepsilon_2\frac{\partial}{\partial t}\nabla^2 T = \frac{\partial^2 \mathrm{T}}{\partial t^2} + \varepsilon_1\frac{\partial^2}{\partial t^2}\psi_1 - E_4\frac{\partial}{\partial t}Q. \tag{26}$$

3 Normal mode analysis

To solve the system of governing equations, the filed variables expressed using the normal mode technique. Each variable is assumed to have the from(Othman [27]):

$$[u_1, u_3, T, \psi_1, \psi_2,, \sigma_{ij}](x,z,t) = [u_1^*, u_3^*, T^*, \psi_1^*, \psi_2^*, \sigma_{ij}^*](z)\exp[i(\omega t + a x)], \tag{27}$$

Where $[u_1^*, u_3^*, T^*, \psi_1^*, \psi_2^*, \sigma_{ij}^*](z)$ *are the amplitudes of the function,* ω *is the complex time constant,* $i = \sqrt{-1}$ *and* a *is the wave number along thex-axis..*

By substituting Eq. (27) into Eqs. (24)-(26), then we have,

$$(\mathrm{D}^2 - F_2)\psi_1^* - F_3\psi_2^* - F_4 T^* = 0, \tag{28}$$

$$\mathrm{F}_5\psi_1^* + (\mathrm{D}^2 - F_6)\,\psi_2^* = 0, \tag{29}$$

$$F_9(\mathrm{D}^2 - a^2)\psi_1^* + (\mathrm{D}^2 - F_{10})T^* = -\mathrm{Q}_0'\mathrm{f}(\mathrm{x},\mathrm{t})\mathrm{e}^{-\gamma z}, \tag{30}$$

Where

$$F_1 = 1 + E_1,\quad F_2 = \frac{F_1 a^2 - E_3(\Omega^2 + \omega^2)}{F_1},\quad F_3 = \frac{2i\,\omega E_3\Omega}{F_1},\ F_4 = \frac{E_2}{F_1},\quad F_5 = 2i\,\omega E_3\Omega,$$

$$F_6 = a^2 - E_3(\omega^2 + \Omega^2),\ F_7 = \varepsilon_1\omega^2,\ F_8 = \varepsilon_3 + \varepsilon_2\omega,\ F_9 = \frac{F_7}{F_8},\ F_{10} = a^2 + \frac{\omega^2}{F_8},\ \mathrm{Q}_0' = \frac{\mathrm{E}_4\mathrm{Q}_0'}{F_8},\ \mathrm{D} = \frac{\mathrm{d}}{\mathrm{dz}}.$$

Eliminating ψ_2^* and T^* between Eqs. (28)-(30), we get the following eighth ordinary differential equation satisfied with ψ_1^*

$$[\mathrm{D}^6 - b_1\mathrm{D}^4 + \mathrm{b}_2\mathrm{D}^2 - \mathrm{b}_3]R^*\psi_1^*(\mathrm{z}) = -J_1\,Q_0'\,f(x,t)\,e^{-\gamma z}, \tag{31}$$

$$[\mathrm{D}^6 - \mathrm{b}_1\mathrm{D}^4 + \mathrm{b}_2\mathrm{D}^2 - \mathrm{b}_3]\psi_2^*(\mathrm{z}) = -J_2\,Q_0'\,f(x,t)\,e^{-\gamma z}, \tag{32}$$

$$[\mathrm{D}^6 - \mathrm{b}_1\mathrm{D}^4 + \mathrm{b}_2\mathrm{D}^2 - \mathrm{b}_3]T^*(\mathrm{z}) = -J_3\,Q_0'\,f(x,t)\,e^{-\gamma z}, \tag{33}$$

Where

$$\mathrm{b}_1 = F_{10} + F_6 + F_2 - F_4F_9,$$

$$\mathrm{b}_2 = F_6F_{10} + F_2F_{10} + F_2F_6 + F_3F_5 - F_4F_6F_9 - F_4F_9a^2,$$

$$b_3 = F_2F_6F_{10} + F_3F_5F_{10} - F_4F_6F_9a^2.$$

Equation (31) can be factored as

$$(\mathrm{D}^2 - k_1^2)(\mathrm{D}^2 - k_2^2)(\mathrm{D}^2 - k_3^2)\psi_1^* = -J_1\,Q_0'\,f(x,t)\,e^{-\gamma z}, \tag{34}$$

published 1-8-2026 تاريخ النشر Accepted 22-7-2026 تاريخ القبول Received 5-7-2026 تاريخ الاستلام

Where, $k_n^2 (n=1,2,3)$ are the roots of the Eq. (31).

The solution of Eq. (31) which is bounded as $z \to \infty$, is given by:

$$\psi_1 = \sum_{n=1}^{3} G_n e^{(-k_n z + i\omega t + iax)} - J_1 g_1 Q_0' f_1(x,t) e^{-\gamma z}, \tag{35}$$

$$\psi_2 = \sum_{n=1}^{3} L_{1n} G_n e^{(-k_n z + i\omega t + iax)} + J_2 g_1 Q_0' f_1(x,t) e^{-\gamma z}, \tag{36}$$

$$T = \sum_{n=1}^{3} L_{2n} G_n e^{(-k_n z + i\omega t + iax)} + J_3 g_1 Q_0' f_1(x,t) e^{-\gamma z}. \tag{37}$$

Where, G_n $(n=1,2,3)$ are some constants.

To obtain the components of the displacement vector, from (35) and (36) in (21)

$$u_1 = \sum_{n=1}^{4} Z_{1n} G_n e^{(-k_n z + i\omega t + iax)} - [\gamma J_2 + \frac{2xJ_1}{r^2}] g_1 Q_0' f_1(x,t) e^{-\gamma z}, \tag{38}$$

$$u_3 = -\sum_{n=1}^{4} Z_{2n} G_n e^{(-k_n z + i\omega t + iax)} + [\frac{2xJ_2}{r^2} - \gamma J_1] g_1 Q_0' f_1(x,t) e^{-\gamma z}, \tag{39}$$

From Eqs. (38),(39) in (19)-(21) to obtain the components of the stresses

$$\sigma_{xx} = \sum_{n=1}^{3} L_{3n} G_n e^{(-k_n z + i\omega t + iax)} + g_1 g_2 Q_0' f_1(x,t) e^{-\gamma z} - g_1 g_3 Q_0' f_2(x,t) e^{-\gamma z}, \tag{40}$$

$$\sigma_{zz} = \sum_{n=1}^{3} L_{4n} G_n e^{(-k_n z + i\omega t + iax)} + g_1 g_4 Q_0' f_1(x,t) e^{-\gamma z} - g_1 g_3 Q_0' f_2(x,t) e^{-\gamma z}, \tag{41}$$

$$\sigma_{xz} = -\sum_{n=1}^{4} L_{5n} G_n e^{(-k_n z + i\omega t + iax)} + g_1 g_5 Q_0' f_1(x,t) e^{-\gamma z}. \tag{42}$$

Where,

$$Z_{1n} = ia - k_n L_{1n}, \quad Z_{2n} = k_n + iaL_{1n}, \quad J_1 = F_4(\gamma^2 - F_6), \; J_2 = -F_4 F_5,$$

$$J_3 = \gamma^4 - (F_2 + F_6)\gamma^2 + F_2 F_6 + F_3 F_5, \quad L_{1n} = \frac{-F_5}{k_n^2 - F_6}, \quad L_{2n} = \frac{(k_n^2 - a^2) - F_3 L_{1n}}{F_4},$$

$$L_{3n} = E_4(iaZ_{1n} + k_n Z_{2n}) + \frac{2iaZ_{1n}}{A^*} - E_5 L_{2n}, \; L_{4n} = E_4(iaZ_{1n} + k_n Z_{2n}) + \frac{2k_n Z_{2n}}{A^*} - E_5 L_{2n},$$

$$L_{5n} = (k_n Z_{1n} + iaZ_{2n}), \; Q_0' = Q_0 f(x,t), \; Q_0 = \frac{I_0 \gamma}{2\pi r^2 t_0^2}, \quad D = \frac{d}{dz},$$

$$f(x,t) = (1 - \frac{t}{t_0}) \exp(\frac{-t}{t_0} - i\omega t - iax - \frac{x^2}{r^2}), \; g_1 = \frac{-1}{\gamma^6 - b_1\gamma^4 + b_2\gamma^2 - b_3},$$

$$g_2 = E_4[\frac{-2J_1}{r^2} - (\frac{2xJ_1}{r^2} + \gamma J_2)(\frac{-2x}{r^2}) - \gamma(\frac{2xJ_2}{r^2} - \gamma J_1)] - \frac{4J_1}{r^2} - (\frac{4xJ_1}{r^2} + 2\gamma J_2)(\frac{-2x}{r^2}),$$

$$g_3 = E_2 J_3, \quad g_4 = E_4[\frac{-2J_1}{r^2} - (\frac{2xJ_1}{r^2} + \gamma J_2)(\frac{-2x}{r^2}) - \gamma(\frac{2xJ_2}{r^2} - \gamma J_1)] - 2\gamma(\frac{2xJ_2}{r^2} - \gamma J_1),$$

$$g_5 = \gamma(\frac{2xJ_1}{r^2} + \gamma J_2) - \gamma(\frac{2xJ_2}{r^2} - \gamma J_1), \quad f_1(x,t) = f(x,t) e^{(\omega t + ikx)}, \quad f_2(x,t) = (1 - \frac{t}{t_0}) e^{(-\frac{x^2}{r^2} - \frac{-t}{t_0})}.$$

published 1-8-2026 تاريخ النشر Accepted 22-7-2026 تاريخ القبول Received 5-7-2026 تاريخ الاستلام

4. Boundary conditions

At the free surface $z=0$ of the half-space, the following conditions are imposed to evaluate the constants G_n for $n=1,2,3$.

Mechanical conditions:

The surface of the half-space is assumed to be subjected to a normal mechanical load and is traction-free in shear:

$$\sigma_{zz}(x,0,t)=-P_1 e^{i(\omega t+ax)}, \qquad (43)$$

$$\sigma_{xz}(x,0,t)=0, \qquad (44)$$

Thermal condition

The surface is also subjected to a prescribed temperature distribution:

$$T(x,0,t)=P_2 e^{i(\omega t+ax)}. \qquad (45)$$

Here P_1 denotes the amplitude of the applied normal force, and P_2 denotes the amplitude of the applied temperature at the boundary.

Using the expressions of the variables into the above boundary conditions (43) - (45) we obtain

$$\sum_{n=1}^{3} L_{4n} G_n = -P_1, \qquad (46)$$

$$-\sum_{n=1}^{3} L_{5n} G_n = 0, \qquad (47)$$

$$\sum_{n=1}^{3} L_{2n} G_n = P_2. \qquad (48)$$

Solving Eqs. (46)-(48) for $G_n\ (n=1,2,3)$ by using the inverse of matrix method as follows

$$\begin{pmatrix} G_1 \\ G_2 \\ G_3 \end{pmatrix} = \begin{pmatrix} L_{41} & L_{42} & L_{43} \\ -L_{51} & -L_{52} & -L_{53} \\ L_{21} & H_{22} & H_{23} \end{pmatrix}^{-1} \begin{pmatrix} -P_1 \\ 0 \\ P_2 \end{pmatrix}. \qquad (49)$$

5. Numerical results

To investigate the behavior of the thermoelastic fields and assess the influence of the governing physical parameters, numerical simulations were performed for a representative material model. The analytical solutions obtained in the previous section were evaluated using the material properties of a magnesium-like isotropic half-space. The physical constants adopted in the numerical computations are listed below(Othman and Edeeb [28]).

مجلة الريادة للبحوث والأنشطة العلمية
Al-Riyadah Journal For Researches And Scientific Activities
العدد الرابع عشر
published 1-8-2026 تاريخ النشر Accepted 22-7-2026 تاريخ القبول Received 5-7-2026 تاريخ الاستلام

$\lambda = 2.17\times10^{10}\ N/m^2,\ \mu = 3.278\times10^{10}\ N/m^2\ K = 1.7\times10^2\ W/m\,\text{deg},$

$\alpha_t = 1.78\times10^{-5} N/m^2,\ \rho = 1.74\times10^3\ kg/m^3, C_E = 1.04\times10^3\ J/kg\,\text{deg},$

$T_0 = 298\,K,\ \beta = 2.68\times10^6 N/m^2\,\text{deg},\ \omega_1^* = 3.58\times10^{11}/s.$

The laser pulse parameters are

$I_0 = 10^5,\quad r = 1\times10^2\ \mu m,\quad \gamma = 1\times10^5\ m^{-1},\quad t_0 = 8\,nan.\text{sec}.$

The comparisons were carried out for

$x = 0.5, t = 0.7, \omega = \zeta_0 + i\,\zeta_1, \zeta_0 = -0.5, \xi_1 = 0.1, p_1 = -0.1, \mathrm{p}_2 = 0.2, a = 0.5, \Omega = 1,$

$\alpha^* = 0.00081, K^* = 85W/mK, 0 \le z \le 25.$

To investigate the effects of time, temperature-dependent material properties, and rotation on the thermoelastic response, three sets of numerical simulations were carried out:

(i) **Effect of time:** The thermoelastic fields were evaluated at two different time instants ($\tau = 0.1\times10^{-13}$, 0.7). The corresponding results are presented in **Figs. 1–6**, illustrating the temporal evolution of the temperature, displacement, and stress distributions.

(ii) **Effect of temperature-dependent material properties:** A comparative study was performed for cases with and without temperature-dependent material properties using two different values of the parameter $(\alpha^* = 0.00081, 0)$, while keeping the remaining parameters fixed. The numerical results are displayed in **Figs. 7–12**.

(iii) **Effect of rotation:** The influence of rotation was examined by comparing the thermoelastic response in the presence and absence of rotation for two different values of the angular velocity ($\Omega = 0.1,\ 0$). The corresponding distributions are illustrated in **Figs. 13–15**.

The material properties presented above were employed to compute the spatial distributions of the thermoelastic fields for the proposed model. The displacement components u_1 and u_3, the temperature distribution T, and the stress components σ_{xx}, σ_{zz} and σ_{xz} were evaluated numerically.

The real parts of these physical quantities are presented graphically in **Figs. 1–15**. The figures provide a comparison between the predictions of the two generalized thermoelastic models considered in this study. In all plots, the **solid** and **dashed** curves correspond to the Green–Naghdi Type II (GN-II) model, whereas the **dotted** curves

مجلة الريادة للبحوث والأنشطة العلمية
Al-Riyadah Journal For Researches
And Scientific Activities
العدد الرابع عشر
published 1-8-2026 تاريخ النشر Accepted 22-7-2026 تاريخ القبول Received 5-7-2026 تاريخ الاستلام

represent the results obtained using the Green–Naghdi Type III (GN-III) model, thereby illustrating the influence of thermal dissipation on the thermoelastic response.

Figs. 1 and 2 illustrate the spatial distributions of the displacement components u_1 and u_3 predicted by the Green–Naghdi Type II (GN-II) and Type III (GN-III) thermoelastic models for two different laser pulse heating times, $\tau = 0.1\times 10^{-13}$, and $\tau = 0.7$. It is observed that both displacement components initially attain negative values and their amplitudes decrease as the laser pulse heating time increases. Furthermore, noticeable differences are observed between the GN-II and GN-III predictions, reflecting the influence of thermal dissipation on the displacement response.

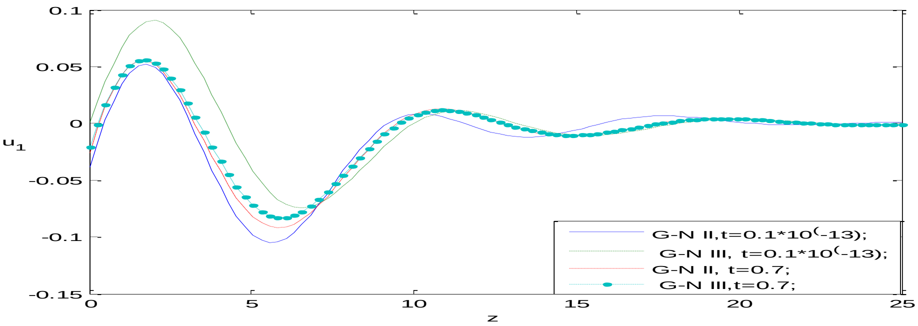

Fig. 1 Distribution of the displacement component u_1 with two values of time.

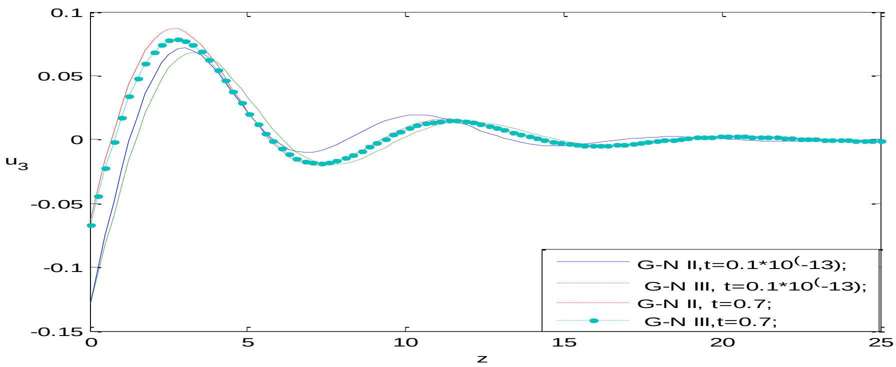

Fig. 2 Distribution of the displacement component u_3 with two values of tim

Fig. 3 presents the spatial distribution of the temperature field T predicted by the Green–Naghdi Type II (GN-II) and Type III (GN-III) thermoelastic models for two different laser pulse heating times, $\tau = 0.1\times 10^{-13}$ and $\tau = 0.7$. The temperature attains its maximum value at the heated surface $z = 0$ and decreases monotonically with increasing depth z, eventually approaching zero. It is also observed that the temperature reaches a higher peak at the earlier time instant, while its amplitude decreases as the laser pulse

مجلة الريادة للبحوث والأنشطة العلمية
Al-Riyadah Journal For Researches And Scientific Activities
العدد الرابع عشر
published 1-8-2026 تاريخ النشر Accepted 22-7-2026 تاريخ القبول Received 5-7-2026 تاريخ الاستلام

heating time increases due to the propagation and diffusion of the thermal wave. Moreover, the GN-II model predicts slightly higher temperature values than the GN-III model, reflecting the effect of thermal dissipation incorporated in the GN-III theory.

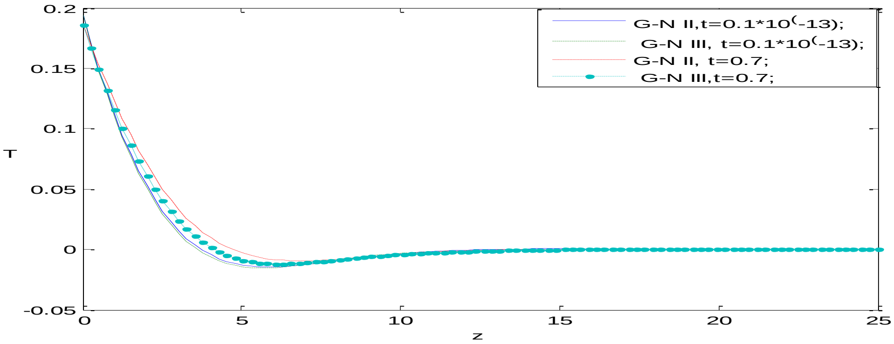

Fig. 3 Temperature distribution *T* with two values of time.

Fig. 4 illustrates the spatial distribution of the normal stress component σ_{xx} predicted by the Green–Naghdi Type II (GN-II) and Type III (GN-III) thermoelastic models for two different laser pulse heating times, $\tau = 0.1 \times 10^{-13}$ and $\tau = 0.7$. The stress component initially assumes negative values, then increases to a positive peak before exhibiting an oscillatory behavior with progressively decreasing amplitude as the distance increases, eventually approaching zero. It is also observed that the magnitude of σ_{xx} decreases with increasing laser pulse heating time. Furthermore, the GN-III model exhibits a faster attenuation of the stress wave than the GN-II model, owing to the thermal dissipation incorporated in the GN-III theory.

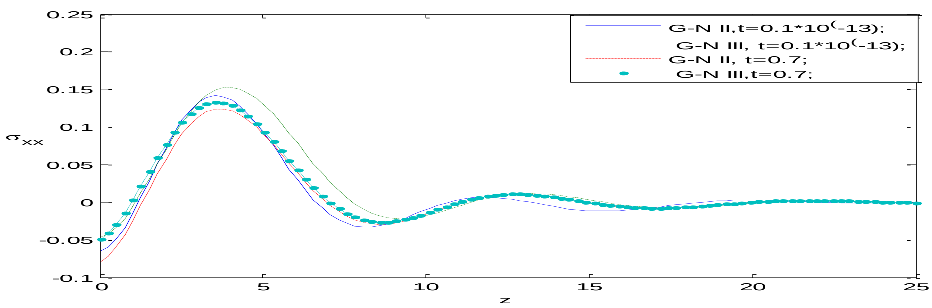

Fig. 4 Distribution of the stress component σ_{xx} with two values of time.

Fig. 5 illustrates the spatial distribution of the stress component σ_{zz} predicted by the Green–Naghdi Type II (GN-II) and Type III (GN-III) thermoelastic models at the specified laser pulse heating time $\tau = 0.1 \times 10^{-13}$ and $\tau = 0.7$. The stress component initially assumes positive values, then decreases to a negative peak before exhibiting an

published 1-8-2026 تاريخ النشر Accepted 22-7-2026 تاريخ القبول Received 5-7-2026 تاريخ الاستلام

oscillatory behavior with diminishing amplitude as the distance increases, eventually approaching zero. It is further observed that the magnitude of σ_{zz} predicted by the GN-II model is greater than that obtained from the GN-III model throughout most of the propagation region. This difference is attributed to the thermal dissipation incorporated in the GN-III theory, which leads to a more pronounced attenuation of the stress waves.

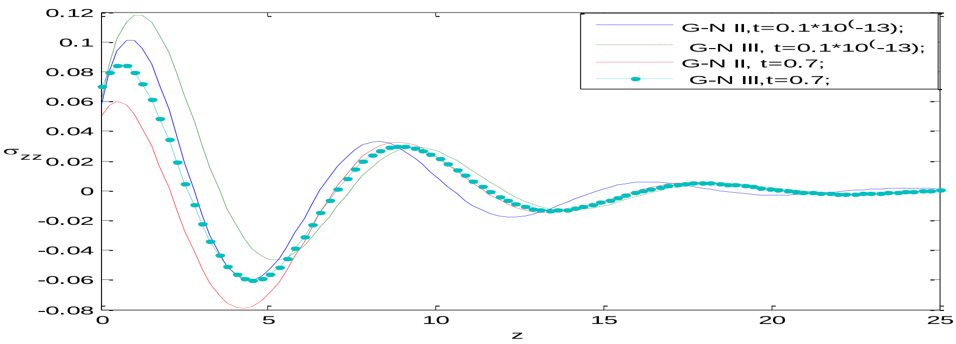

Fig. 5 Distribution of the stress component σ_{zz} with two values of time.

Fig. 6 presents the distribution of the shear stress component σ_{xz} obtained from the Green–Naghdi Type II (GN-II) and Type III (GN-III) thermoelastic models for two different laser pulse heating times, $\tau = 0.1 \times 10^{-13}$ and $\tau = 0.7$. It is observed that the shear stress initially starts from zero, decreases to a negative minimum value, and then exhibits an oscillatory behavior with gradually decreasing amplitude until it approaches zero. The magnitude of the shear stress decreases as the laser heating time increases. Moreover, the GN-II model predicts higher values of σ_{xz} compared with the GN-III model, indicating that the thermal dissipation effect included in the GN-III theory results in stronger attenuation of the shear stress waves.

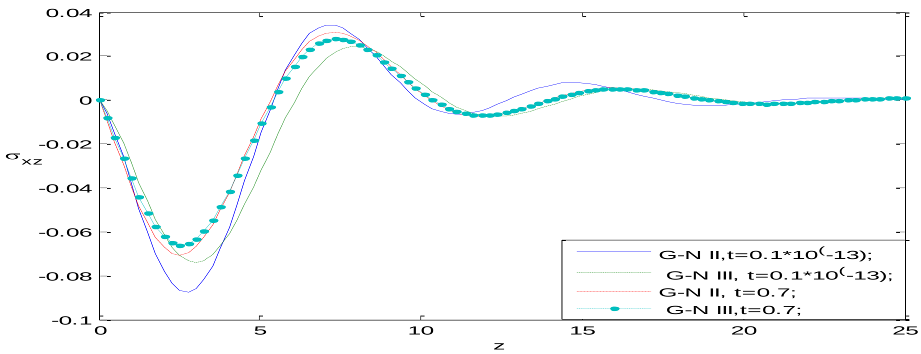

Fig. 6 Distribution of the stress component σ_{xz} with two values of time.

مجلة الريادة للبحوث والأنشطة العلمية
Al-Riyadah Journal For Researches And Scientific Activities
العدد الرابع عشر
published 1-8-2026 تاريخ النشر Accepted 22-7-2026 تاريخ القبول Received 5-7-2026 تاريخ الاستلام

Figs. 7 and 8 illustrate the distributions of the displacement components u_1 and u_3 predicted by the Green–Naghdi Type II (GN-II) and Type III (GN-III) models for two different values of the temperature-dependent parameter $\alpha^* = 0.00081$ and $\alpha^* = 0$. It is observed that both displacement components exhibit oscillatory behavior with gradually decreasing amplitudes as the distance z increases. Furthermore, the magnitudes of u_1 and u_3 decrease with increasing values of α^* for $z > 0$, indicating the significant influence of temperature-dependent material properties on the displacement fields.

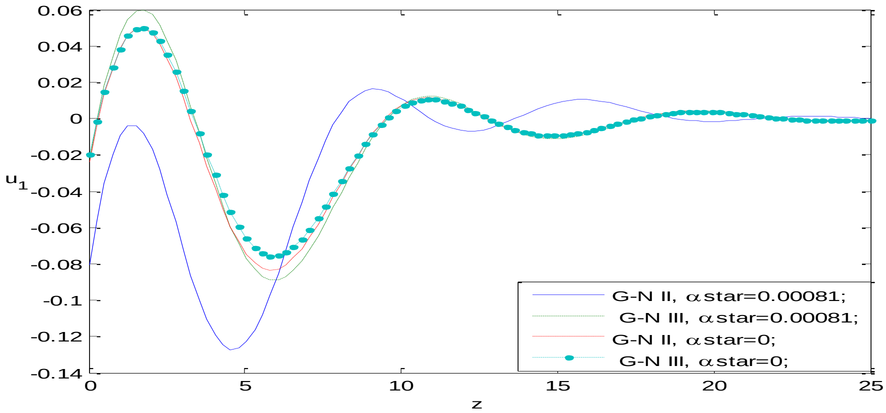

Fig. 7 Distribution of the displacement component u_1 with two values of time

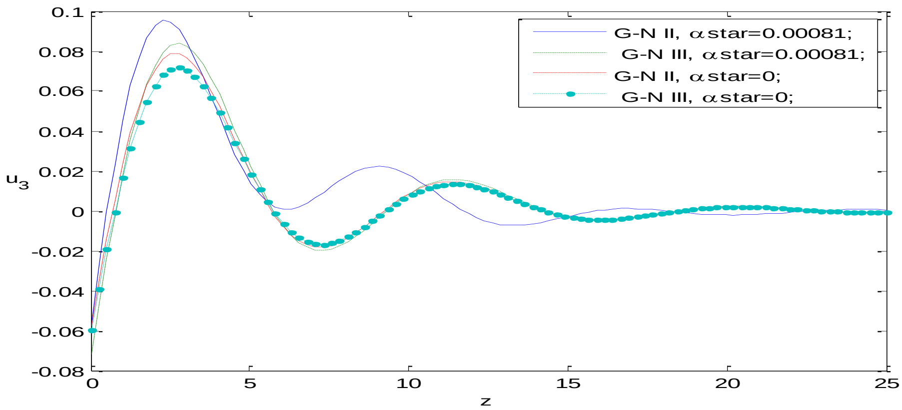

.

Fig. 8 Distribution of the displacement component u_3 with two values of time.

Fig. 9 depicts the distribution of the thermodynamic temperature T for different values of the temperature-dependent parameter $\alpha^* = 0.00081$ and $\alpha^* = 0$. It is observed that the temperature field begins with positive values and satisfies the prescribed boundary conditions at the surface $z = 0$. Furthermore, for $\alpha^* = 0.00081$ and $\alpha^* = 0$ the

مجلة الريادة للبحوث والأنشطة العلمية
Al-Riyadah Journal For Researches And Scientific Activities
العدد الرابع عشر
published 1-8-2026 تاريخ النشر Accepted 22-7-2026 تاريخ القبول Received 5-7-2026 تاريخ الاستلام

temperature distribution increases as the temperature-dependent parameter is varied, demonstrating the significant effect of temperature-dependent material properties on the thermal response of the medium.

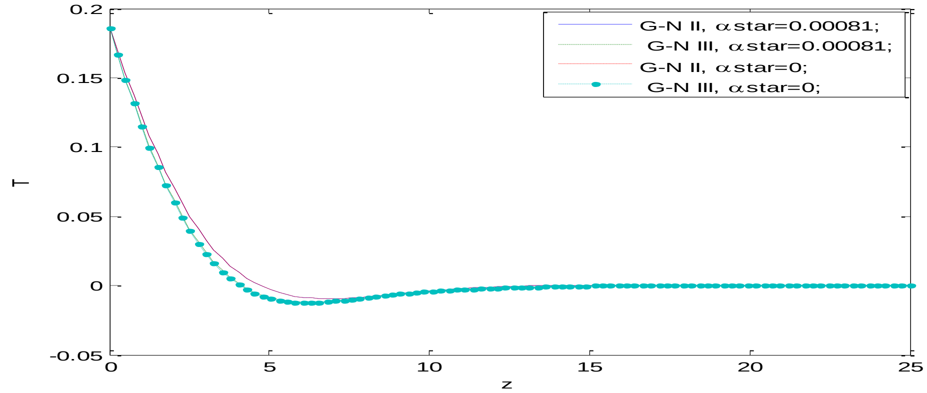

Fig.9 Temperature distribution T with two values of time.

Fig. 10 presents the distribution of the stress component σ_{xx} obtained using the Green–Naghdi Type II (GN-II) and Type III (GN-III) models for two different values of the temperature-dependent parameter, $\alpha^* = 0.00081$ and $\alpha^* = 0$. It is observed that the stress component σ_{xx} initially increases, reaches a maximum peak value, and then gradually decreases with increasing distance z. Furthermore, the magnitude of σ_{xx} increases as the parameter α^* increases for $z > 0$, indicating the significant influence of temperature-dependent material properties on the stress distribution.

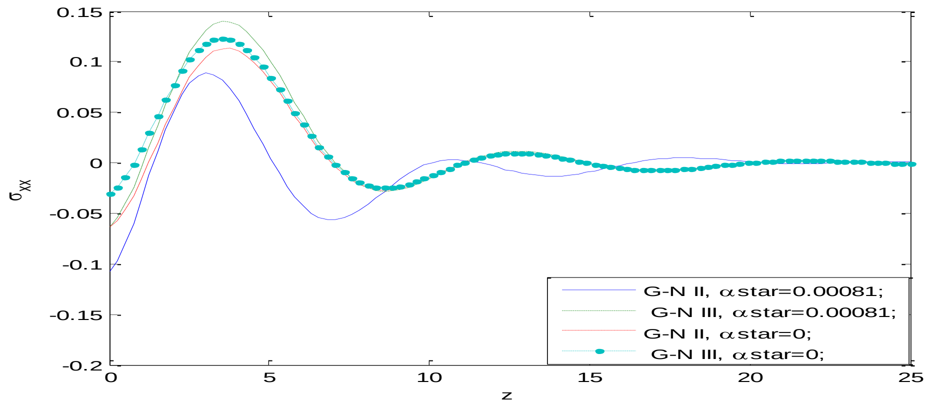

Fig. 10 Distribution of the stress component σ_{xx} with two values of time.

Fig. 11 illustrates the distribution of the stress component σ_{zz} predicted by the Green–Naghdi Type II (GN-II) and Type III (GN-III) models for two different values of the

مجلة الريادة للبحوث والأنشطة العلمية
Al-Riyadah Journal For Researches And Scientific Activities
العدد الرابع عشر
published 1-8-2026 تاريخ النشر Accepted 22-7-2026 تاريخ القبول Received 5-7-2026 تاريخ الاستلام

temperature-dependent parameter, $\alpha^* = 0.00081$ and $\alpha^* = 0$. It is observed that the stress component σ_{zz} initially starts from a positive value and satisfies the prescribed boundary conditions. Furthermore, the magnitude of σ_{zz} decreases and then increases as the value of α^* is varied, demonstrating the significant effect of temperature-dependent material properties on the stress response.

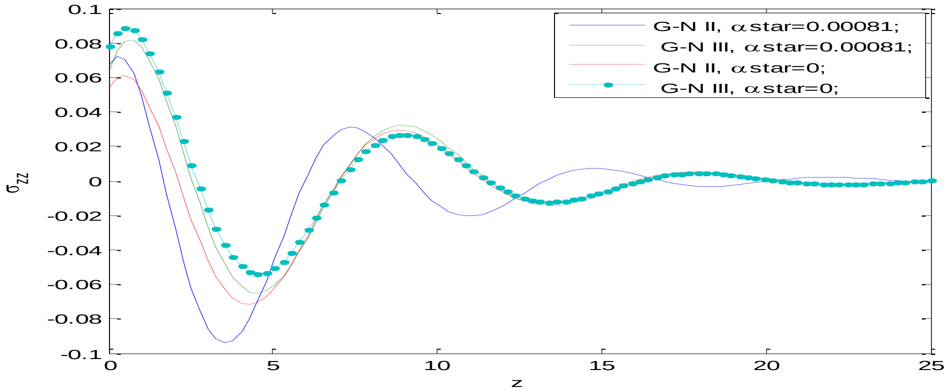

Fig. 11 Distribution of the stress component σ_{zz} with two values of time.

Fig. 12 presents the distribution of the shear stress component σ_{xz} obtained from the Green–Naghdi Type II (GN-II) and Type III (GN-III) models for two different values of the temperature-dependent parameter, $\alpha^* = 0.00081$ and $\alpha^* = 0$. It is observed that the shear stress exhibits an oscillatory behavior with gradually decreasing amplitude as the distance z increases, eventually approaching zero. Moreover, the magnitude of σ_{xz} increases with increasing values of the parameter α^* for z, indicating the significant influence of temperature-dependent material properties on the shear stress distribution.

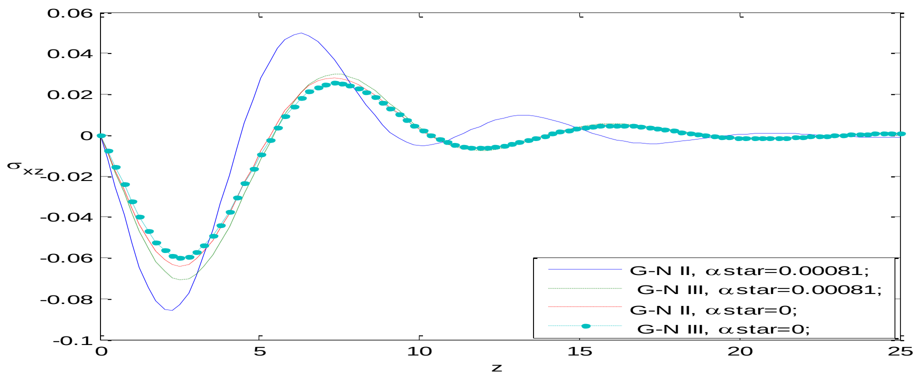

Fig. 12 Distribution of the stress component σ_{xz} with two values of time.

مجلة الريادة للبحوث والأنشطة العلمية
Al-Riyadah Journal For Researches And Scientific Activities
العدد الرابع عشر
published 1-8-2026 تاريخ النشر Accepted 22-7-2026 تاريخ القبول Received 5-7-2026 تاريخ الاستلام

Figs.13 and 14 illustrate the distributions of the displacement components u_1 and u_3 predicted by the Green–Naghdi Type II (GN-II) and Type III (GN-III) models for two different rotation parameters, $\Omega = 0.1$, and $\Omega = 0$. It is observed that both displacement components exhibit oscillatory behavior with gradually decreasing amplitudes as the distance z increases.For the displacement component u_1, the curves corresponding to both rotational cases begin with positive values at $z = 0$ and its magnitude decreases as the rotation parameter increases, indicating the significant influence of rotational effects on the displacement field.Similarly, the displacement component u_3 shows a decaying oscillatory pattern with increasing z . For the non-rotating case $\Omega = 0$, the curves start from zero and satisfy the prescribed boundary conditions, whereas for the rotating case $\Omega = 0.1$, the curves begin with positive values. The amplitude of u_3 decreases with increasing rotation, demonstrating the suppressing effect of rotational motion on the displacement response.

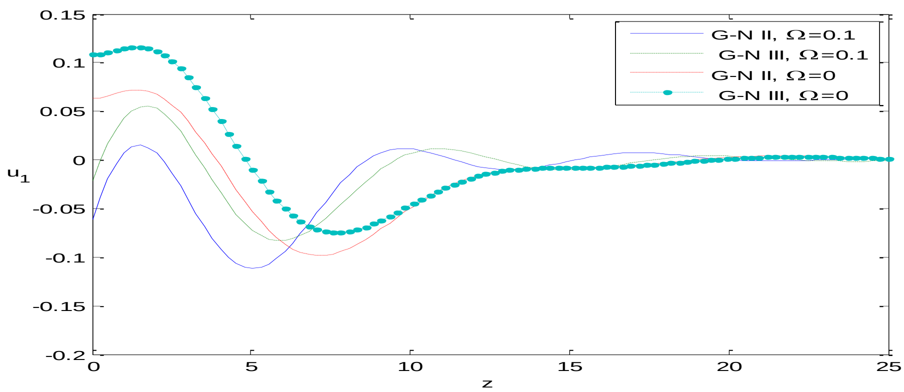

Fig. 13 Horizontal displacement distribution u_1 in the absence and presence of rotation

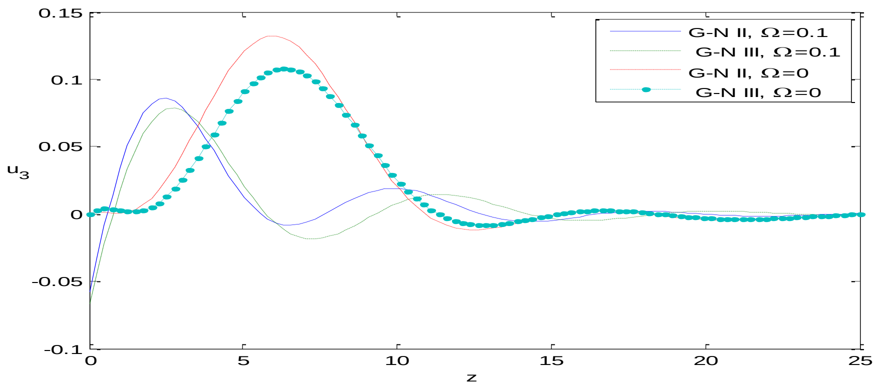

Fig.14 Vertical displacement distribution u_3 in the absence and presence of rotation

مجلة الريادة للبحوث والأنشطة العلمية
Al-Riyadah Journal For Researches And Scientific Activities
العدد الرابع عشر
published 1-8-2026 تاريخ النشر Accepted 22-7-2026 تاريخ القبول Received 5-7-2026 تاريخ الاستلام

Fig. 15 illustrates the distribution of the shear stress component σ_{xz} predicted by the Green–Naghdi Type II (GN-II) and Type III (GN-III) models for two different rotation parameters, $\Omega = 0.1$, and $\Omega = 0$. It is observed that the shear stress component σ_{xz} starts from zero at $z = 0$, satisfying the prescribed boundary conditions for all cases. As the distance z increases, σ_{xz} exhibits an oscillatory behavior with gradually decreasing amplitude. Furthermore, the magnitude of σ_{xz} decreases with increasing rotation parameter Ω. The results also indicate that the values predicted by the GN-II model are slightly higher than those obtained from the GN-III model for the non-rotating case $\Omega = 0$, due to the absence of thermal dissipation effects in the GN-II formulation.

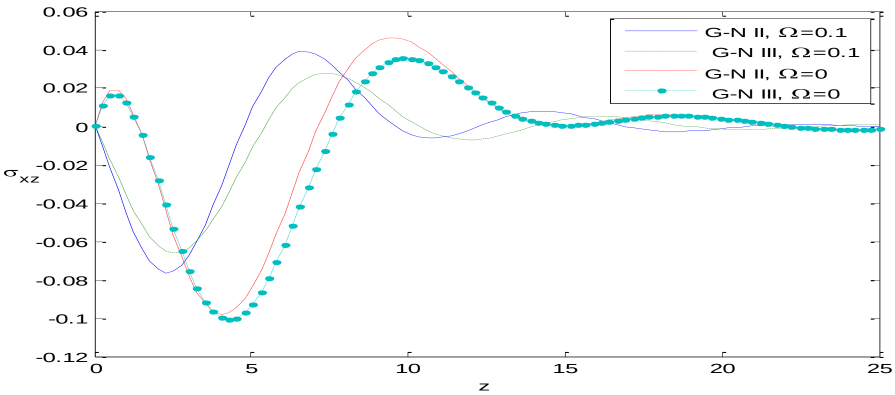

Fig. 15 Distribution of stress component σ_{xz} in the absence and presence of rotation.

The three-dimensional distributions shown in **Figs. 16–21** represent the complete dependence of the thermoelastic fields on both spatial coordinates x and z. These results are obtained for the Green–Naghdi Type III (GN-III) model in the presence of rotation $\Omega = 0.1$, temperature-dependent properties $\alpha^{*} = 0.00081$ and laser pulse thermal loading with intensity $I_0 = 10^5$ at time $t = 0.08$. These figures provide a comprehensive illustration of the variation of the physical quantities throughout the medium and demonstrate their dependence on the vertical distance from the origin. It is observed that all field quantities propagate as thermoelastic waves with amplitudes gradually decreasing as the distance z increases. Moreover, the magnitude of the physical fields is reduced with increasing rotation parameter Ω, indicating the significant influence of rotational effects on the wave propagation behavior.

مجلة الريادة للبحوث والأنشطة العلمية
Al-Riyadah Journal For Researches
And Scientific Activities
العدد الرابع عشر

published 1-8-2026 تاريخ النشر   Accepted 22-7-2026 تاريخ القبول   Received 5-7-2026 تاريخ الاستلام

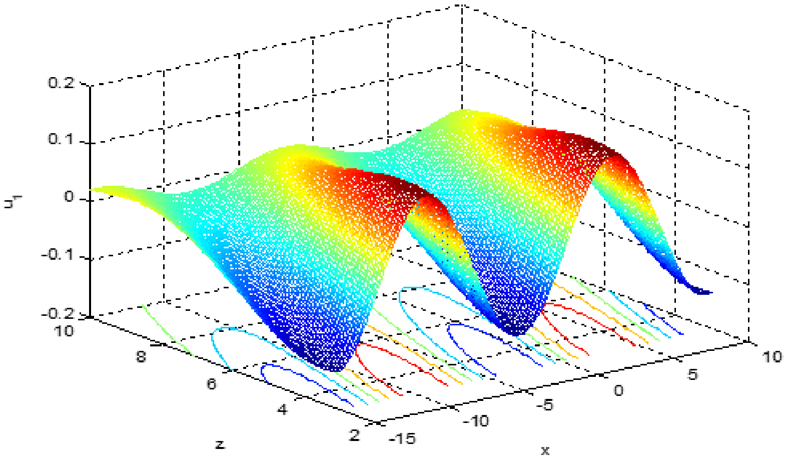

Fig. 16. 3D variation of the displacement u_1 with the variation of x , z .

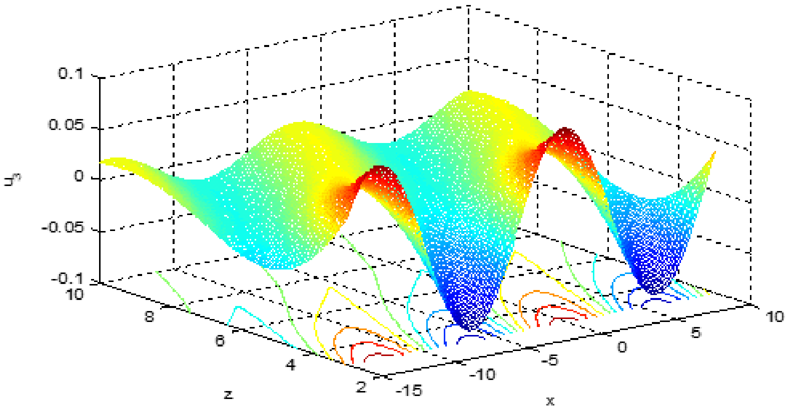

Fig. 17. 3D variation of the displacement u_3 with the variation of x , z.

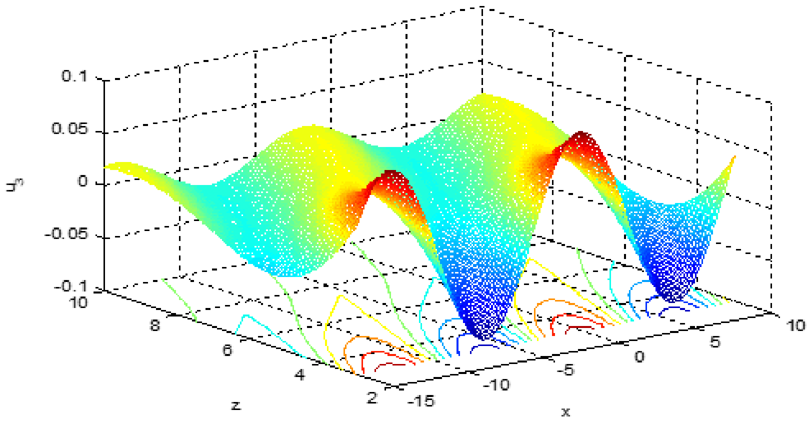

Fig. 17. 3D variation of the displacement u_3 with the variation of x , z .

مجلة الريادة للبحوث والأنشطة العلمية
Al-Riyadah Journal For Researches
And Scientific Activities
العدد الرابع عشر
published 1-8-2026 تاريخ النشر Accepted 22-7-2026 تاريخ القبول Received 5-7-2026 تاريخ الاستلام

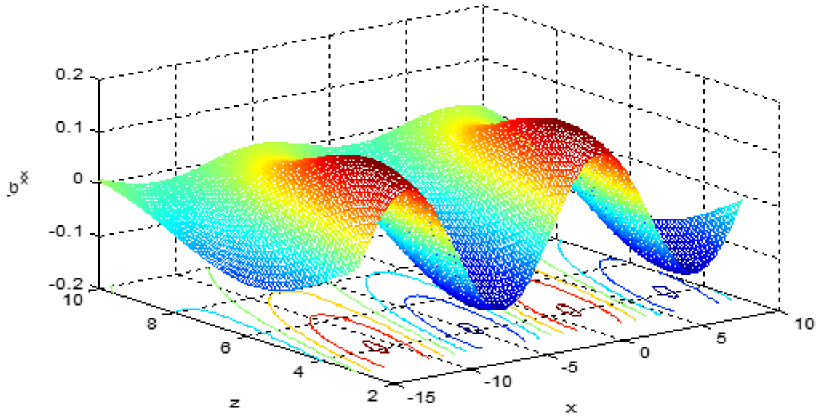

Fig. 19. 3D variation of the stress distribution σ_{xx} with the variation of x , z .

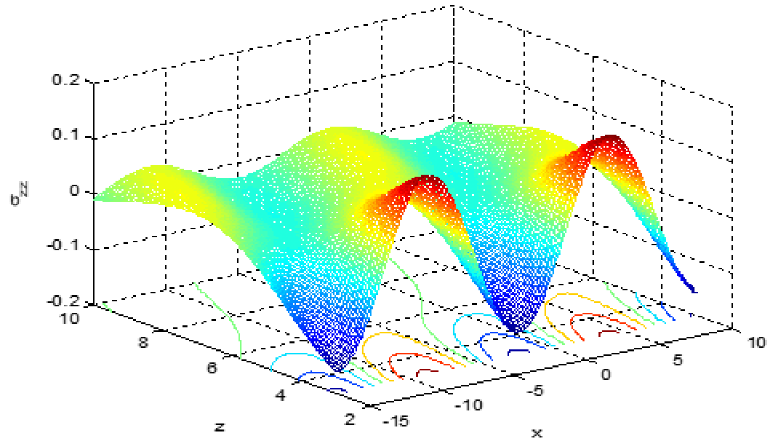

Fig. 20. 3D variation of the stress distribution σ_{zz} with the variation of x .

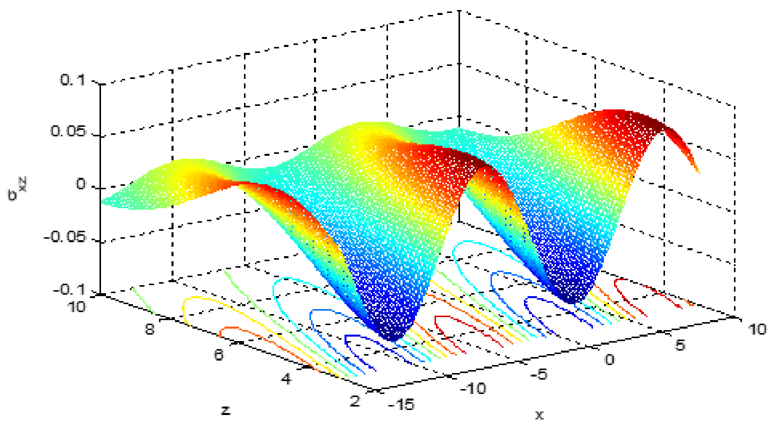

Fig. 21. 3D variation of the stress distribution σ_{xz} with the variation of x , z .

published 1-8-2026 تاريخ النشر Accepted 22-7-2026 تاريخ القبول Received 5-7-2026 تاريخ الاستلام

6. Conclusions

Based on the theoretical analysis and numerical results presented in this study, the following conclusions can be drawn:

* The Green–Naghdi Type III (GN-III) model produces thermoelastic responses that differ significantly from those predicted by the Green–Naghdi Type II (GN-II) model under identical loading and material conditions, highlighting the influence of thermal dissipation on wave propagation.

* All physical quantities, including temperature, displacement, and stress components, decrease gradually with increasing depth in the half-space and eventually approach zero, satisfying the physical boundary conditions and demonstrating the continuity of the obtained solutions.

* The rotational parameter has a pronounced influence on the thermoelastic fields. Increasing the rotation rate reduces the amplitudes of the temperature, displacement, and stress distributions, indicating that rotation significantly alters wave propagation characteristics.

* Temperature-dependent material properties have a substantial effect on the thermo-elastic response. Variations in these properties modify the magnitudes and distributions of the displacement, temperature, and stress fields, emphasizing the importance of accounting for material nonlinearity in thermoelastic analyses.

* The ultra-short laser pulse generates transient thermoelastic waves whose amplitudes decay as the propagation distance increases. The laser-induced thermal loading strongly affects the evolution of the temperature and stress fields, particularly during the early stages of wave propagation.

* The overall thermoelastic behavior of the rotating half-space is governed by the combined effects of laser pulse heating, rotational motion, temperature-dependent material properties, and the selected Green–Naghdi thermoelastic model.

* The analytical approach based on the normal mode method provides an efficient and accurate framework for solving generalized thermoelastic problems involving rotation, laser pulse heating, and variable material properties. The present formulation can be extended to investigate more complex thermoelastic models and engineering applications involving advanced functional materials and laser–matter interactions.

published 1-8-2026 تاريخ النشر Accepted 22-7-2026 تاريخ القبول Received 5-7-2026 تاريخ الاستلام

Conflicts of interests: On behalf of all authors, the corresponding author states that there is no conflict of interests.

Data availability: Data sharing is not applicable to this paper as no data sets were created or analyzed during the current investigation.

Funding: The author(s) received no financial support for the research, authorship, and/or publication of this article.

Author Contribution: Alzaerah R.M. Aldeeb, Mohamed I.A. Othman, wrote the main manuscript text and prepared figures 1-21. All authors reviewed the manuscript.

References

1. Othman,M.I.A., Hasona, W.M. and Eraki, E.E.M.(2014). "The effect of initial stress on generalized thermoelastic medium with three-phase-lag model under temperature-dependent properties".Canadian Journal of Physics 92(5), 448-4571. 2. 2 .Hetnarski, R.B. and Eslami, M.R. (2020). "Thermal Stresses-Advanced Theory and Applications". Springer.

3. Othman,M.I.A. and Said, S.M.(2012). "The effect of rotation on two-dimensional problem of a fiber-reinforced thermoelastic with one relaxation time" International Journal of Thermophysics 33(2), 160-171.

4. Othman, M.I.A., Said, S.M., and Gamal, E.M. (2024). "Eigenvalue approach on a fiber-reinforced magneto-visco-thermoelastic rotating medium with initial stress". Journal of Vibration Engineering & Technologies, **12**(3), 5173-5187.

5. Green, A.E. and Naghdi, P.M. (1991). "A re-examination of the basic postulates of thermo-mechanics". Proceedings of the Royal Society A,London 432, 171-194.

6. Green,A.E. and Naghdi, P.M.(1993)."Thermoelasticity without energy dissipation" Journal of Elasticity, 31, 189-208.

7. Abbas, I.A. (2021). "Generalized thermoelasticity in an infinite medium with GN theory". Mechanics Based Design of Structures and Machines, 49(4), 512-527.

8. Hobiny, A. and Abbas, I. (2023). "GN-II and GN-III models for porous media under thermal shock". Case Studies in Thermal Engineering, 45, 102921.

9. Singh, B. and Kaur, J. (2022). "Thermoelastic interactions in a rotating solid due to thermal shock". Materials Physics and Mechanics, 48(3), 321-334.

published 1-8-2026 تاريخ النشر Accepted 22-7-2026 تاريخ القبول Received 5-7-2026 تاريخ الاستلام

10. Abo-Dahab, S.M. (2020). "Rotation and initial stress effect on thermoelasticity with GN theory". Steel and Composite Structures, 35(6), 789-798.

11. Lotfy, K. and El-Bary, A.A. (2024)." Effect of rotation and temperature-dependent properties on generalized thermoelastic medium". Journal of Computational and Applied Mechanics, 19(1), 45-60.

12. Zenkour, A.M. (2022). "Thermoelastic interaction in rotating media with temperature-dependent properties based on GN model". Acta Mechanica, 233(5), 1891-1906.

13. Sherief, H.H. and El-Sayed, A.M. (2021). "Two-temperature GN model for thermoelastic problems". Continuum Mechanics and Thermodynamics, 33, 1541-1555.

14. Lata, P. and Kaur, I. (2024). "Effect of magnetic field and rotation in GN thermoelastic solid". Waves in Random and Complex Media, 34(1), 234-250.

15. Youssef, H.M. and Al-Lehaibi, E.A. (2023). "Generalized thermoelasticity problem of a solid sphere under laser pulse". Waves in Random and Complex Media, 33(2), 456-471.

16. Mondol, S. and Mukhopadhyay, S. (2021). "Thermoelastic response of a rotating elastic medium due to laser pulse". International Journal of Mechanical Sciences, 192, 106123.

17. Sharma, N. and Grover, D. (2025)." Thermoelastic analysis of rotating disks under laser heating". Applied Mathematical Modelling, 138, 115623.

18. Kumar, R. and Devi, S. (2024). "Laser pulse effect on thermoelastic medium using GN-III model". Journal of Thermal Analysis and Calorimetry, 149, 1123-1135.

19. Othman, M.I.A. and Kumar, R. (2021). "Response of thermoelastic solid due to thermal loading via GN-III theory". Journal of Thermal Stresses, 44(3), 245-259.

20. Ezzat, M.A. (2020). 'Thermoelectric MHD with memory-dependent derivatives". International Journal of Engineering Science, 155, 103256.

21. Schoenberg M. and Censor D., (1973)."Elastic waves in rotating media". Quart. Appl. Math., **31**, 115-125.

22. Othman, M.I.A. and Abd-Elaziz, E.M. (2017). "Plane Waves in a magneto-thermoelastic solids with voids and microtemperatures due to hall current and rotation".Results in Physics 7, 4253-4263.

published 1-8-2026 تاريخ النشر Accepted 22-7-2026 تاريخ القبول Received 5-7-2026 تاريخ الاستلام

23. Othman, M.I.A. and Atwa, S. Y. (2014). "Effect of rotation on a fiber-reinforced thermoelastic under Green-Naghdi theory and influence of gravity". Meccanica 49 (1), 23-36.

24. Sarkar, N., Mondal, S. and Othman, M.I.A. (2020). "Effect of the laser pulse on transient waves in a nonlocal thermoelastic medium under Green-Naghdi theory".Structural Engineering and Mechanics, An Int. J. 74(4), 471-479.

25. Othman, M.I.A. and Edeeb, E.R.M. (2012). "2-D problem of a rotating thermo-elastic solid with voids and thermal loading due to laser pulse under three theories". Journalof Computational and Theoretical Nanoscience 13(1), 294-305.

26. Othman, M.I.A. and Edeeb, E.R.M. (2018). "The Effect of rotation on thermo- elastic medium with voids and temperature dependent under three theories". Journal of Engineering Mechanics 144(3), 04018003-1-14.

27. Othman, M.I.A. (2003). "State-space approach to generalized thermoelasticity plane waves with two relaxation times under dependence of the modulus of elasticity on reference temperature". Canadian Journal of Physics 81(12), 1403-1418.

28. Othman, M.I.A. and Edeeb, E.R.M. (2021). "Effect of rotation on plane waves of generalized magneto-thermoelastic medium with voids under thermal loading due to laser pulse". Applications and Applied Mathematics: An Int. J. 16(2), 1077-1098.